Space frequency analysis of microscope images by 2-dimensional fast Fourier transform

Kyoichi OSHIDA* and Tatsuo NAKAZAWA**

The practical image analysis method for the microscope pictures of electrical materials is introduced. The frequency analysis of the digitized TEM pictures by using a 2-dimensional (2D) fast Fourier transform (FFT) and the real space images reconstruction by means of the 2D inverse FFT (IFFT) are mentioned. The concrete picture image reconstruction method by 2D-IFFT is illustrated.

Key words: Transmission electron microscopy, Image analysis, Fast Fourier transform, Graphite intercalation compounds

1. Introduction

The study of the microstructure of electronic materials can be enhanced by using high resolution transmission electron microscopy (TEM) combined with image analysis. The digital image analysis method can apply to quantitative investigation of the microscope picture. As shown in Fig.1, the techniques of digital image processing for microscope images are divided roughly into two categories of methods. One (the upper side flow in the Fig.1) is a spatial frequency analysis by the 2-dimensional (2D) fast Fourier transform (FFT), and the verification by the 2D inverse FFT (IFFT). Another (the down side flow in the Fig.1) is the measurement and the outline extraction on the bases of the binarized microscope picture image.

In this paper, we have shown the practical image analysis method for the microstructures of acceptor graphite intercalation compounds (GICs) with $CuCl_2$

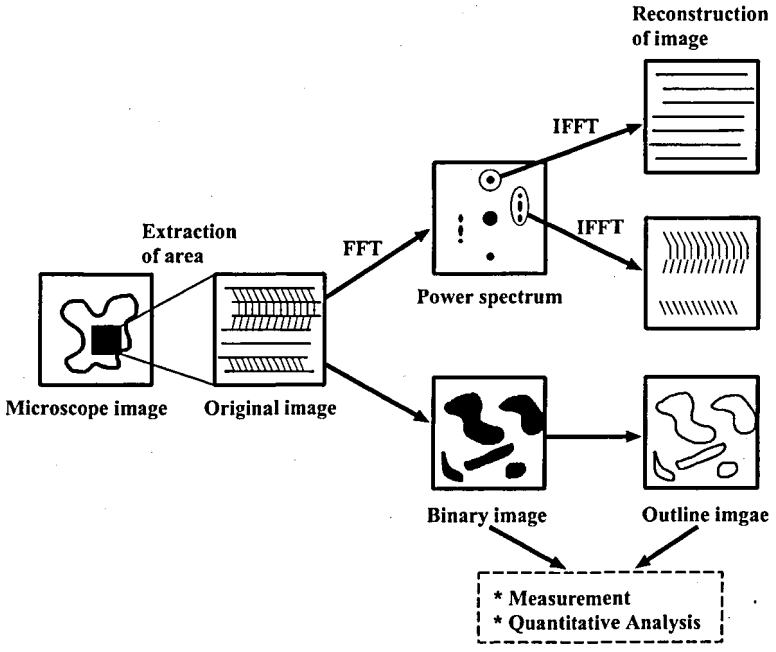

Fig. 1. The flow of the image analysis.

* Associate Professor, Department electronics and computer science
** Professor, Department electronics and computer science
Received October 31, 2000

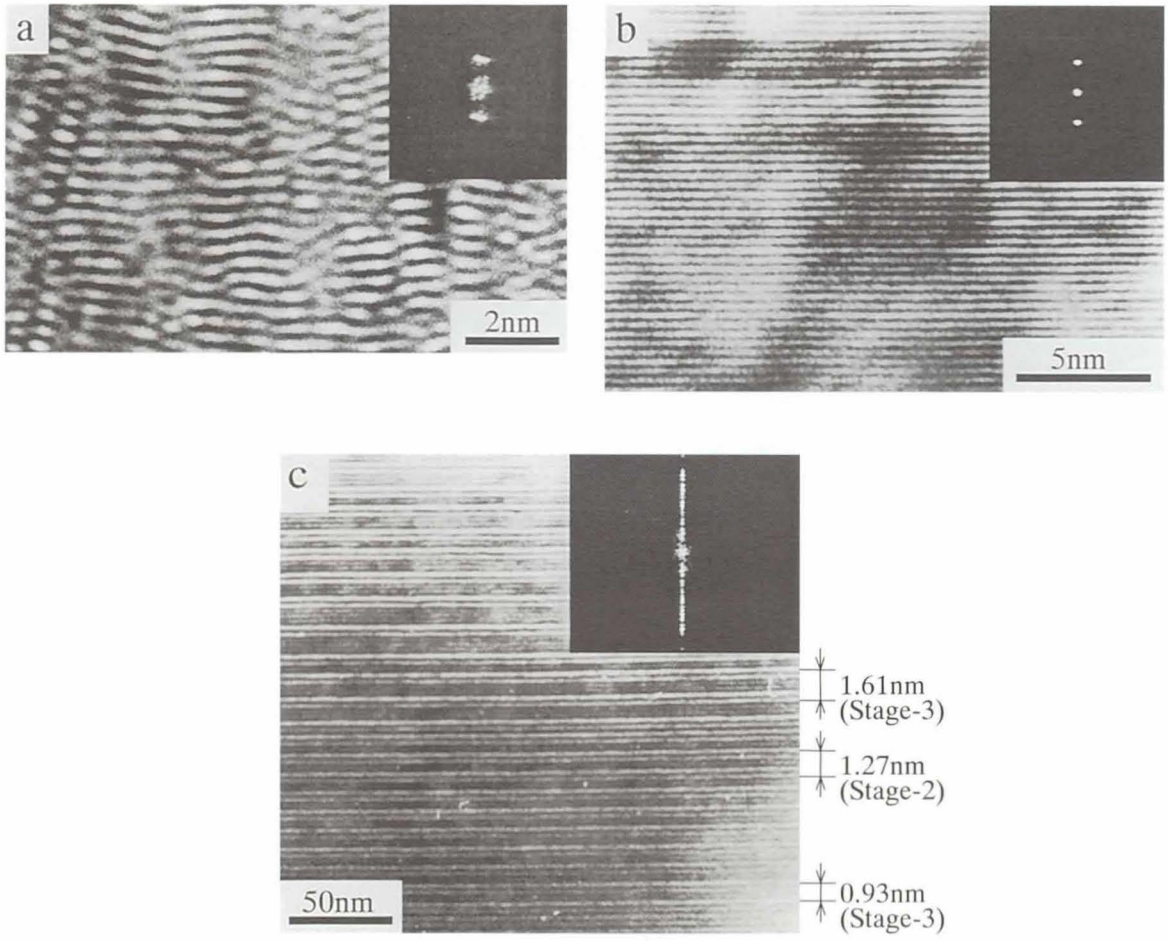

Fig. 2. Lattice fringe images of a precursor VGCF sample (a), a pristine VGCF sample heat treated to 2900°C (b), and a $CuCl_2$ intercalated VGCF sample. The corresponding power spectra obtained form the digitized images of them by 2D-FFT are shown in the insets, respectively.

intercalants. The 2D-FFT was used for the frequency analysis of the TEM pictures. From the analysis of the power spectrum obtained by the 2D-FFT, some specific frequencies and real space images associated with these frequencies were extracted by means of the 2D-IFFT.

2. Frequency analysis

The TEM images of the lattice fringes for precursor vapor grown carbon fibers (VGCFs)[1),2)], of pristine VGCFs heat-treated to 2900°C and of $CuCl_2$ intercalated VGCF are shown in Fig.2 (a), (b) and (c), respectively[3),4)]. In order to prepare the digital data for the successive analysis, these TEM images were digitized and store in the computer. The digitized images are called as the original images from here.

The 2D-FFT/-IFFT is the operation to the whole image, and different from the partial operation like Laplacian filter, that is, the 2D-FFT can remove periodic noises and distortions of the whole image that cannot be eliminated by the partial operation. Furthermore, it is possible to do space frequency analysis of the whole image. The process of 2D-FFT and 2D-IFFT operations are shown in Fig.3. The result of FFT is the complex number, and the power spectrum is calculated by the sum of each square of the real part and the imaginary part. Since the TEM image itself is thought to be window, which cut down the continuous data to the rectangular, the edge of the image is discontinuous and it affects the characteristics of resulting power spectrum. In order to remove this effect, the window treatment is performed to the original image before the FFT operation. In this study, we use Hamming window for the window treatment. A series of window treatment, FFT, power spectrum process is shown in the upper flow of Fig.3, while a series of FFT,

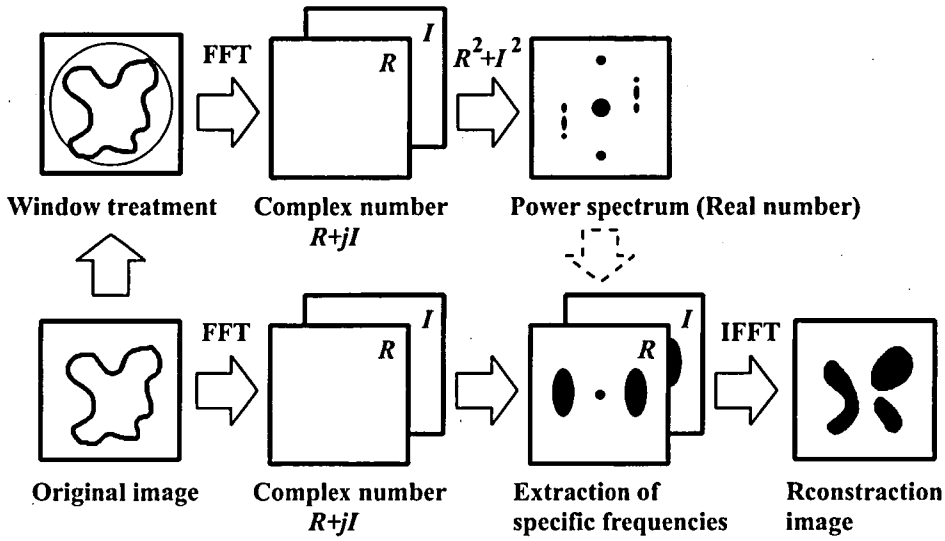

Fig.3. The 2 dimensional fast Fourier transform (2D-FFT) and the 2 dimensional inverse fast Fourier transform (2D-IFFT) operation.

extraction specific frequencies, IFFT process is the down flow in Fig.3. On the other hand, the window treatment is not need when we get the reconstruction image by IFFT operation. The specific frequencies are estimated by analysis of the power spectrum, and the mask pattern is made for the extraction of specific frequencies. The mask pattern is applied to the complex data calculated by the FFT operation without window treatment, then the specific frequency image is obtained by the IFFT operation.

The insets of each picture in Fig.2 are the power spectra of the original images obtained by the 2D-FFT[5]. The two bright spots in the power spectrum of Fig.2 (b), that are symmetrically positioned about the central point, correspond to the 002 lattice planes. The central point corresponds to the brightness of the original image. Since the two 002 spots and the center spot appear to be sharp, it is known that the 002 lattice planes are consistently parallel and the interlayer spacing is uniform. In comparison, the spots in the power spectrum, which correspond to the 002 lattice planes in Fig.2 (a) are extended. The extension of the spots along the x-axis indicates the presence of a perturbation to the 002 lattice planes, whereas the extension along the y-axis corresponds to a spread in the distribution of interlayer spacings.

The extended size of the spots in Fig.2 (a) especially along the x-axis, relative to those in Fig.2 (b), indicates that the structure of the precursor VGCFs is more disordered than that of the heat-treated VGCFs. Located near the center of the power spectrum in Fig.2 (b) is a cloud of spots. The cloud indicates the existence of a change in the magnitude at long spatial intervals in the principal direction appearing in the image. The size of the diffuse spots provides a measure of the size of the regions with a similar orientation, and of the different orientations of lattice planes within the lattice image under analysis. All the lattice planes in Fig.2 (b) have a common direction.

Figure 2 (c) shows the lattice fringe images for $CuCl_2$ intercalated VGCFs with the inset indicating its power spectrum obtained by the 2D-FFT. The pattern, which appears in the power spectrum, is very similar to the streaking, found in the electron diffraction pattern of the same sample. We can thus obtain the streak pattern either by image analysis, or by electron diffraction. Its characteristic pattern is distributed in a line perpendicular to the 00*l* lattice planes of the original image. The spectrum is very sharp for $CuCl_2$ GICs and this is because the transverse width of the FFT power spectrum pattern is very small, indicating large lateral regions with the same stage. Since the spectrum is distributed only in one direction, the 2-dimensional power spectrum image can be graphed by integration perpendicular to the distribution of the spectrum[5], using the same approach as was followed for the TEM images of the pristine VGCFs and of the

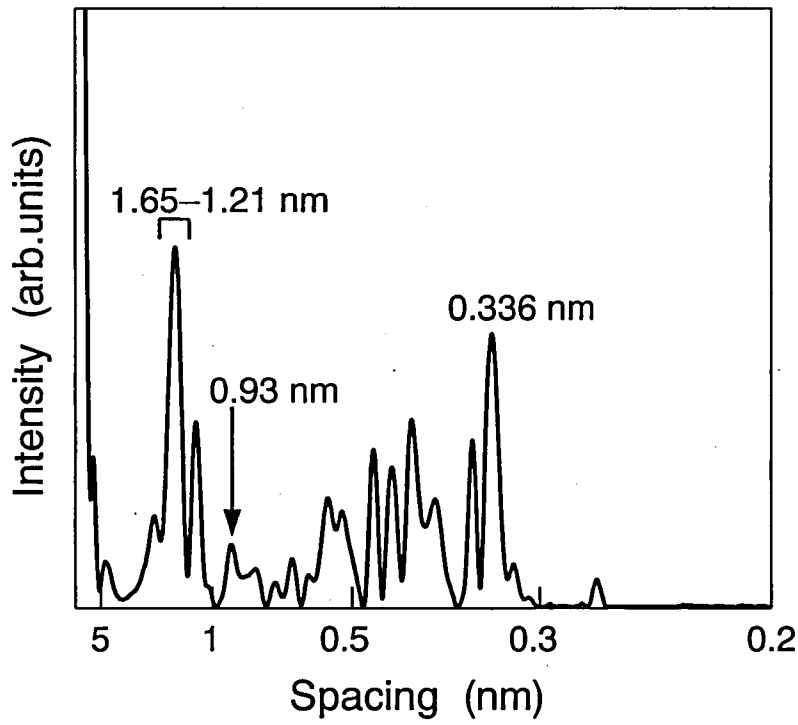

Fig. 4. The distribution of interlayer repeat distances for the $CuCl_2$ intercalated VGCF sample obtained from the power spectrum of Fig. 2 (c).

VGCFs heat-treated to 2900°C.

Figure 4 shows the distribution of interlayer spacings obtained by integration along the x-axis of the power spectrum in Fig.2(c). There are many peaks in the integrated power spectrum in Fig.4 in the region between 0.3 and 4 nm. The large peak on the right at 0.336 nm corresponds to the 002 graphite lattice planes. Stage-1, stage-2, and higher stage regions as well as graphite stacking are assumed to appear in Fig.4. We observe a fairly small stage-1 peak around 0.93 nm. There is another peak between 1.21 and 1.65 nm (the highest point located at 1.396 nm). This peak is thought to consist of a stage-2 component (peak at 1.27 nm) and a stage-3 component (peak at 1.61 nm).

From this frequency analysis, it is clear that the TEM pattern for $CuCl_2$ GICs shows evidence of stage-1, stage-2, and stage-3 regions, and graphite stacking, but the presence of the stage-1 region is not as evident in the original image shown in Fig.2(c) as in the Fourier analysis in Fig.4. There are several other peaks between the graphite and stage-1 peaks which may contribute to the construction of the original image.

These peaks have the possibility of containing the following two kinds of components. One is a fundamental component from which the shape of the wave is formed, and the other one is associated with harmonic components. Since the brightness of the TEM image of the $CuCl_2$ GICs changes smoothly, a very low intensity for the harmonic components is expected, except for the harmonic component of the 002 lattice planes, as mentioned above. It may be that the components in the real space image are related to these peaks.

Some of the image components cancel one another, which causes dark spaces to appear in the image for the $CuCl_2$ intercalated layers, while some other components reinforce each other, and contribute to the shape of the stage layers. It appears that the streak in the power spectrum of Fig.2(c) consists of a series of peaks superimposed on the power spectrum.

3. Reconstruction of the image

Real space images were reconstructed by taking the 2D-IFFT in order to verify the staging structure of the $CuCl_2$ VGCFs discussed above. The images reconstructed from the specific frequencies corresponding to the interlayer spacings of 0.336nm and 1.396nm are shown in

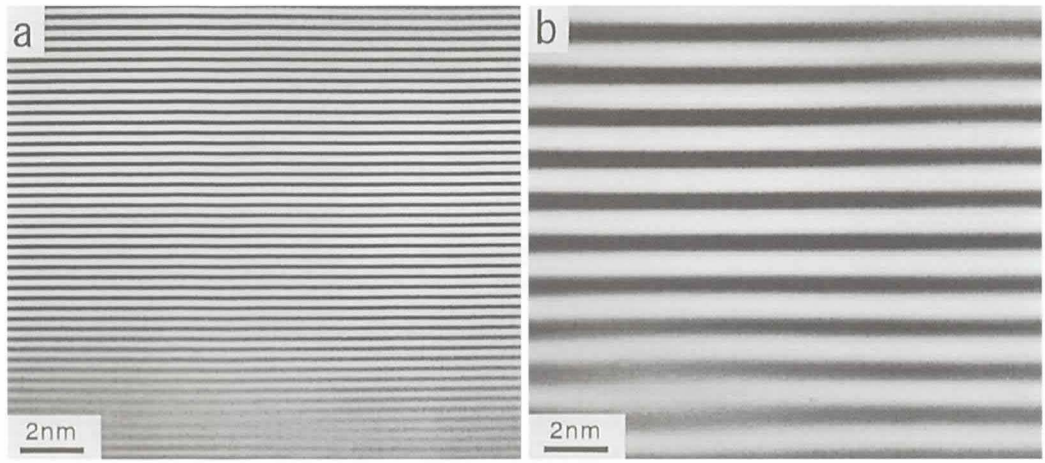

Figs. 5. Images of IFFT for a $CuCl_2$ intercalated VGCF sample. The images are reconstructed from specific frequencies corresponding to the interlayer spacings of (a) 0.336nm and (b) 1.396nm.

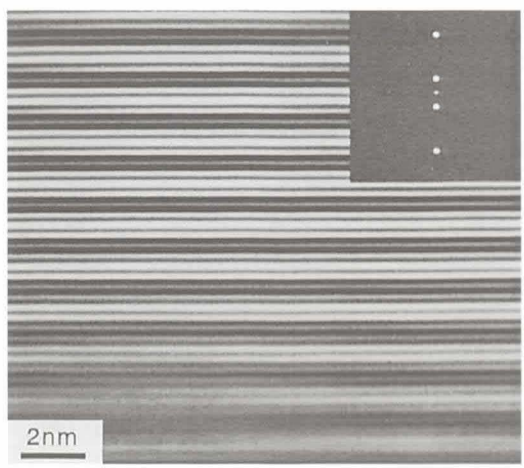

Fig. 6. Image of the IFFT for the $CuCl_2$ intercalated VGCF sample corresponding to the superposition two interlayer spacings, 0.336nm and 1.396nm.

Fig.5 (a) and (b), respectively[6),7)]. The white lines in Fig.5 (a) correspond to the 002 lattice fringe, and those in Fig.5 (b) correspond to the stage-2 or stage-3 regions in the interlayer image. The images of Fig.5 (a) and (b) are easily superimposed upon each other by selecting the specific frequencies and then performing the 2D-IFFT. The figure obtained by superimposing Figs.5(a) and (b) by this method is shown in Fig.6. The inset to Fig.6 shows the selected area pattern of the power spectrum that is used for the extraction of the specific frequencies in the image pattern. The central points of the power brightness of the real space image. In Fig.6, we find that an image similar to the stage image of GICs can be constructed from two different frequencies corresponding to the high intensity peaks in the power spectrum. But the superimposed image (Fig.6) differs slightly from the original image shown in Fig.2(c), which may contain stage-1, -2, -3 regions.

The other frequency components are hypothesized to contribute to the construction of the original image. We were able to reconstruct the corresponding images shown in Fig.7 by taking the FFT of the IFFT. The images in Fig.7 are centered on peaks at (a) 0.358nm, (b) 0.412nm, (c) 0.443nm, and (d) 0.478nm of the power spectrum shown in Fig.4. The peaks appear between the graphite and stage-1 interlayer spacings. The brightness of the images is modulated, respectively, for clear viewing. We can see that the spacings of the layers are slightly extended on going from (a) to (d) in Fig.7 Figure 8 (b) is the image obtained by superimposing Figs.5 (a), (b), and Figs.7 (a) to (d). The original TEM image of $CuCl_2$ (Fig.2 (c)) is shown again in Fig.8 (a) in comparison with (b). We can see that Fig.8 (b) is more similar to the original image than Fig.6. The layers of Fig.8 (b) appear to be sharper than those in the original image (a) because the selection of specific frequencies acts as a noise reduction operation. But some lines appear in faint form in the $CuCl_2$ intercalated layers of Fig.2 (c). This appearance is caused by a lack of data when the specific frequencies were selected. If all of the frequencies present in the original image (Fig.2 (c)) can be identified and selected, a perfect reconstruction of the original image can be achieved.

However, the original image of Fig.8 (a) already contains some faint lines where the intercalants enter and

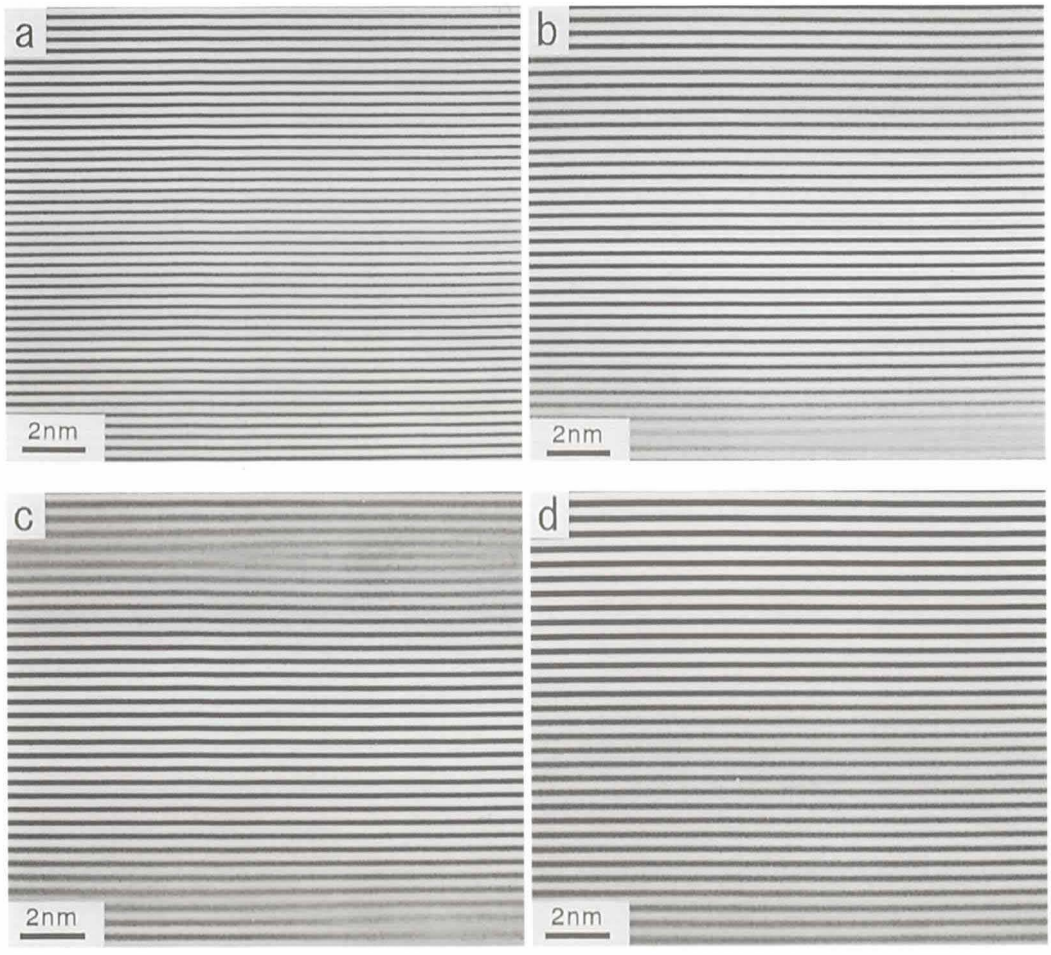

Figs. 7. Image of the IFFT for the $CuCl_2$ intercalated VGCF sample. The images are reconstructed from the specific frequencies corresponding to the interlayer spacings of (a) 0.358nm, (b) 0.412nm, (c) 0.443nm and (d) 0.478nm.

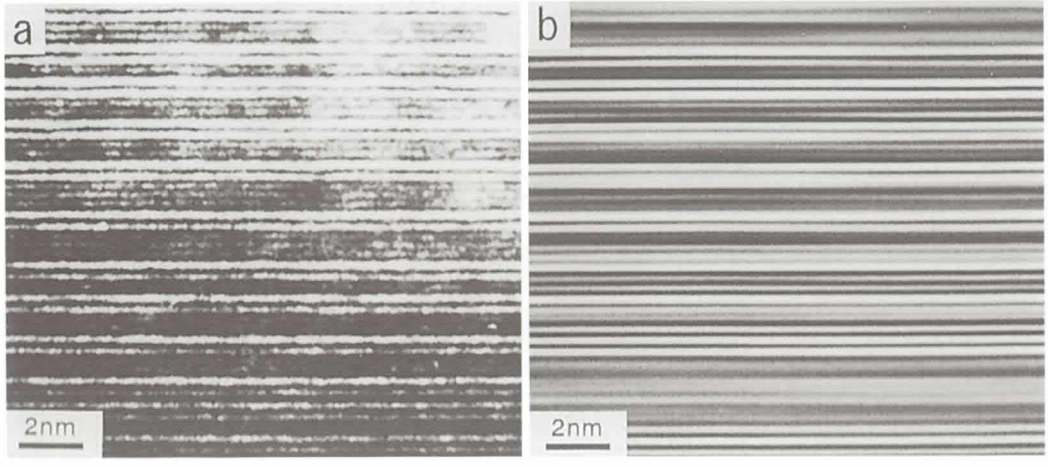

Figs. 8. (a) Original lattice fringe image of the $CuCl_2$ intercalated VGCF sample. (b) Image of the IFFT for the $CuCl_2$ intercalated VGCF sample reconstructed from all specific frequencies shown in Figs. 5 and 7.

exit. These faint features appear as a result of the influence of the aperture setting when the TEM image was taken, which occurred likewise when the above image analysis, the specific frequency selection of the power spectrum, were made. A part of the electron beam of TEM is intercepted by the aperture. Therefore the aperture setting of TEM observation may also acts as a frequency 3selection of the electron diffraction.

As a result of these analyses, it is clear that the lattice fringe image of the $CuCl_2$ GIC (Fig.2(c)) consists of certain images which correspond to specific frequencies that are revealed by analysis of the power spectrum, where stage-2 and stage-3 images are shown to be dominant in the 00*l* graphite lattice fringe image. Images which correspond to the other interlayer spacings present further details that are found in the original stage image.

4. Summary

The practical image analysis method for the microscope pictures of electrical materials were introduced. The frequency analysis of the digitized TEM pictures was done by using a 2-dimensional (2D) fast Fourier transform (FFT). Real space images were reconstructed successfully by means of the 2D inverse FFT (IFFT) using some specific frequencies obtained from the analysis result of the power spectrum obtained by the 2D-FFT. It is thought that the analytical method of spatial frequency analysis according to a 2D-FFT and verification by the reconstruction of the picture image using 2D-IFFT is useful to the material research.

Acknowledgment

The work by the author (KO) is supported by a grant-in-aid for "Re-search for the Future" Program No. JSPS-RFTF96R11701 from the Japan Society for the Promotion of Science.

References

1) M. Endo: Grow carbon fibers in the vapor phase, *Chemtech*, American Chemical Society, Vol.18, pp.568-576 (1988).
2) T. Koyama, M. Endo et al.: Carbon fibers obtained by thermal decomposition of vaporized hydrocarbon, *Jpn. J. Appl. Phys.*, Vol.11, No.4, pp.445-449, 1972.
3) M. Endo, T. C. Chieu, G. Timp, and M. S. Dresselhaus: Properties of acceptor intercalation graphite fibers, *Synth. Metals*, Vol.8, pp.251-260 (1983).
4) M. Endo, T. C. Chieu, G. Timp, M. S. Dresselhaus, and B. S. Elman: Stractural and electrical porperties of intercalated and ion-implanted highly ordered graphite fibers, *Phys. Rev.* B, Vol.28, No.12, pp.6982-6991 (1983).
5) K. Oshida, M. Endo, T. Nakajima, S. L. di Vittorio, M. S. Dresselhaus, and G. Dresselhaus: mage analysis of TEM picture of fluorine-intercalated graphite fibers, *J. Mater. Res.*, Vol.8, No.3, pp.512-522 (1993).
6) M. Endo, K. Oshida, K. Kobori, K. Takeuchi, K. Takahashi, and M. S. Dresselhaus: Evidence for glide and rotation defects observed in well-ordered graphite fibers, *J. Mater. Res.*, Vol.10, No.6, pp.1461-1468 (1995).
7) K. Oshida, K. Kogiso, K. Matsubayashi, K. Takeuchi, S. Kobori, M. Endo, M. S. Dresselhaus, and G. Dresselhaus: Analysis of pore structure of activated carbon fibers using high resolution transmission electron microscopy and image processing, *J. Mater. Res.*, Vol.10, No.10, pp.2507-2517 (1995).